Published in final edited form as:
Dev Biol. 2007 January 1; 301(1): 82–91.

The 14-3-3 protein FTT-2 regulates DAF-16 in *Caenorhabditis elegans*

Ji Li[1], **Muneesh Tewari**[2,3], **Marc Vidal**[2], and **Siu Sylvia Lee**[1]

1 *Department of Molecular Biology, Cornell University, Ithaca, NY 14850*

2 *Center for Cancer Systems Biology (CCSB) and Department of Cancer Biology, Dana-Farber Cancer Institute, and Department of Genetics, Harvard Medical School, Boston, MA 02115*

3 *Fred Hutchinson Cancer Research Center, Human Biology Division, Seattle, WA, 98109*

Abstract

The *C. elegans daf-2*/insulin-like signaling pathway is critical for regulating development, longevity, metabolism and stress resistance. We identified the 14-3-3 protein FTT-2 to be a new regulatory component of this pathway. We found that RNAi knock down of *ftt-2* specifically enhanced the *daf-2*-mediated dauer formation phenotype. Furthermore, *ftt-2* knock down caused the nuclear accumulation of DAF-16/FOXO, the forkhead transcription factor that is the major downstream effecter of *daf-2*/insulin-like signaling, and enhanced the transcriptional activities of DAF-16. In contrast to *ftt-2*, RNAi knock down of *par-5/ftt-1*, the only other gene predicted to encode a 14-3-3 protein in *C. elegans*, did not show any notable effect on dauer formation, DAF-16 localization, or DAF-16 downstream gene transcription, underscoring the functional specification of FTT-2 and PAR-5 despite their high sequence homology. Using co-immunoprecipitation, we revealed that FTT-2 formed a complex with GFP-fused DAF-16 in *C. elegans*. Our results indicate that FTT-2 binds to DAF-16 in *C. elegans* and regulates DAF-16 by sequestering it in the cytoplasm. A similar mechanism of regulation of FOXO by 14-3-3ζ has been reported in mammalian cells, highlighting the high degree of conservation of the *daf-2*/insulin-like signaling pathway.

Keywords

14-3-3; *ftt-2*; *par-5*; *daf-16*; FOXO; *daf-2*; insulin signaling

Introduction

C. elegans daf-16 encodes a forkhead transcription factor (FOXO) that regulates many biological processes, including dauer formation (Riddle and Albert, 1997), lifespan (Lin et al., 1997;Ogg et al., 1997), reproduction (Gems et al., 1998), and fat accumulation (Kimura et al., 1997). DAF-16 is the major downstream effecter of the *daf-2*/insulin-like signaling pathway. When the *daf-2*/insulin-like signaling pathway is activated, the transmembrane receptor protein tyrosine kinase DAF-2 triggers the activation of the downstream phosphatidylinositol 3- kinase AGE-1 and the protein kinase B/AKT, which leads to phosphorylation of DAF-16 and retention of DAF-16 in the cytoplasm (Brunet et al., 1999). When *daf-2*/insulin-like signaling is reduced or inactivated, DAF-16 becomes dephosphorylated and migrates into the nucleus to affect gene

Correspondence should be addressed to: Siu Sylvia Lee, Email: SSL29@cornell.edu, Phone: 607-255-8015, Fax: 607-255-6249

expression (Halaschek-Wiener et al., 2005;Lin et al., 2001;McElwee et al., 2003;Murphy et al., 2003). Interestingly, reduced *daf-2*/insulin-like signaling in *C. elegans* results in constitutive dauer formation (Kenyon et al., 1993;Kimura et al., 1997;Riddle et al., 1981) and dramatic lifespan extension (Kenyon et al., 1993) phenotypes that are completely dependent on *daf-16* (Gottlieb and Ruvkun, 1994;Larsen et al., 1995). Therefore, nuclear translocation and eventual activation of DAF-16 likely induces gene expression changes that promote dauer formation and longevity extension (Halaschek-Wiener et al., 2005;Lee et al., 2003a;McElwee et al., 2003;Murphy et al., 2003).

The *daf-2* pathway in *C. elegans* is entirely orthologous to the insulin/IGF-1 signaling pathways in fruit flies and mammals (Clancy et al., 2001;Holzenberger et al., 2003;Tatar et al., 2001). Three mammalian DAF-16 orthologs (FOXO1, FOXO3a and FOXO4) have been characterized to regulate apoptosis, oxidative stress response, DNA repair, and metabolism (Birkenkamp and Coffer, 2003). In mammalian cultured cells, the subcellular localization of FOXO3a is regulated by binding to the 14-3-3ζ protein. When FOXO3a is phosphorylated by protein kinase B/Akt, it is bound by 14-3-3ζ and sequestered in the cytoplasm (Brunet et al., 1999). Since the insulin/IGF-1 signaling pathway is highly conserved, it is possible that *C. elegans* DAF-16 is also regulated by a similar mechanism.

14-3-3 proteins are a family of highly conserved, abundant cytoplasmic proteins identified in all eukaryotic organisms examined. They are small (~30 kD), acidic proteins that usually function as hetero or homo-dimers (Jones et al., 1995). In general, 14-3-3 proteins bind to the phosphorylated form of substrate proteins. A large number of proteins are found to contain a consensus 14-3-3 recognition motif: RSXpSXP or RXXXpSXP (Yaffe et al., 1997), in which the phosphorylated serine is essential for binding (Pozuelo Rubio et al., 2004). However, 14-3-3 proteins are also capable of binding to several unphosphorylated ligands (Masters et al., 1999). By binding to their substrates, 14-3-3 proteins can induce the conformational change of the substrate proteins (Obsil et al., 2001;Yaffe, 2002), or sequester the substrate proteins in the cytoplasm (Grozinger and Schreiber, 2000), or act as a scaffold that bridges two interacting partners (Agarwal-Mawal et al., 2003). By binding to a diverse group of signaling molecules, such as Raf -1 (Fu et al., 1994;Irie et al., 1994), Cdc25 phosphatase family members (Chen et al., 2003;Forrest and Gabrielli, 2001;Peng et al., 1997) and Bad (Datta et al., 2000), 14-3-3 proteins are thought to participate in a wide variety of cellular processes, including cell cycle checkpoints, DNA repair, cell differentiation and apoptosis (Fu et al., 2000). 14-3-3 proteins typically have several isoforms in one given organism. For example, there are seven known isoforms in mammals (Ichimura et al., 1988;Martin et al., 1993) and thirteen in Arabidopsis (DeLille et al., 2001). In *C. elegans*, two 14-3-3 encoding genes have been identified: *par-5*/*ftt-1* and *ftt-2* (Wang and Shakes, 1996). *par-5* is required for cellular asymmetry in the early *C. elegans* embryo. PAR-5 regulates the asymmetric cortical localization of PAR-1 and PAR-2 to the posterior and PAR-3, PAR-6 and PKC-3 to the anterior (Morton et al., 2002). Until recently, the function and protein substrates of FTT-2 were not known (Berdichevsky et al., 2006;Wang et al., 2006).

Using gene-specific RNAi knock down, we show that the *C. elegans* 14-3-3 protein FTT-2 regulates DAF-16 activities by forming a protein complex with DAF-16 and preventing DAF-16 from entering the nucleus to regulate transcription. Our results indicate that the DAF-16 sub-cellular localization is regulated by a conserved mechanism similar to that of FOXO in mammalian cells. In contrast to *ftt-2*, *par-5*, the only other gene predicted to encode a 14-3-3-like protein in *C. elegans*, has no effect on dauer formation, DAF-16 localization or DAF-16 transcriptional activities, highlighting the functional specification of two highly homologous 14-3-3 members.

Materials and Methods

Strains and maintenance

The strains used in this paper were as follow: wild type N2 (from the *C. elegans* Genetic Center), *daf-16 (mgDf47), rrf-3(pk1426), daf-2 (e1370), daf-16(mgDf47)*; xrls87 [*daf-16a::gfp*::DAF-16B, *rol-6*(su1006)], *daf-2(e1370); daf-16(mgDf47)*; xrls87 [*daf-16a::gfp*::DAF-16B, *rol-6*(su1006)], muIs84[pAD76*(sod-3::gfp)*]. All strains were maintained on NGM plates seeded with *Escherichia coli* OP50 as the food source.

Construction of *ftt-2* and *par-5* specific RNAi constructs

The sequences corresponding to the 3′ end and 3′UTR of the predicted *ftt-2* and *par-5* transcripts were amplified from genomic DNA of N2 worms by PCR. The primers used for the *par-5* RNAi construct: Forward primer: 5′-tggacatctgacgttggagctga -3′; Reverse primer: 5′-ggaatgacaatagtgacggagtga -3′. The primers used for the *ftt-2* RNAi construct: Forward primer: 5′-acgctgccaccgatgacactg -3′; Reverse primer: 5′-aaggggggaaaagccgtaacaaaa -3′. The *ftt-2* primers and the *par-5* forward primer are kind gifts from the Kemphues lab (K. Kemphues, Cornell University, Ithaca NY). The RNAi constructs were generated by inserting the *ftt-2* or *par-5* PCR products into the L4440 vector (a kind gift from Dr. A. Fire, Stanford). The RNAi plasmids were transformed into *Escherichia coli* HT115 (Timmons et al., 2001) for feeding RNAi experiments. All other feeding RNAi clones have been described previously (Lee et al., 2003b).

RNA interference

Feeding RNAi was performed as described (Lee et al., 2003b). Briefly, RNAi bacteria were grown in Luria both with 50 μg ml^{-1} ampicillin at 37°C for 10–16 hrs, seeded onto NGM plates containing 2mM IPTG, and induced at room temperature overnight.

Dauer assay

Dauer assay for *daf-2(e1370)* strain was performed as described (Lee et al., 2003b). *daf-2 (e1370)* (Gems et al., 1998) worms at the L4 stage were put onto RNAi plates and allowed to lay egg over night. The resulting self-progeny were allowed to develop at 22°C. At ~96 hrs after egg lay, the number of dauers and adult worms on each plate were scored. Five plates were scored for each RNAi treatment. Dauer assay for N2 or *rrf-3(pk1426)* strain was performed at 25°C and the number of dauers in each population was scored at ~ 72 hrs after egg lay. The dauer assays were repeated three times.

DAF-16::GFP localization assay

The construction and characterization of the *daf-16(mgDf47)*; xrls87[*daf-16a::gfp*::DAF-16B, *rol-6*(su1006)] transgenic strain have been described (Lee et al., 2001). DAF-16::GFP transgenic worms at the L4 stage were put onto the RNAi bacteria and allowed to lay egg at 16°C over night. Self-progeny were allowed to develop on the RNAi bacteria at 16°C till they were at the L3 stage. The worms were cultured at 16°C to allow for a longer time for RNAi to take effect before the worms reached the L3 stage for scoring. The GFP expression of the DAF-16::GFP worms feeding on the various RNAi bacteria was monitored using a fluorescent microscope (Leica MZFL III) and images were captured using a Hamamatsu ORCA-ER camera and OpenLab software.

Lifespan assay

Unless stated otherwise, lifespan assays were performed at 22°C. N2 or *daf-2(e1370)* L4 larvae worms were allowed to lay egg over night on RNAi plates and the progeny grew on RNAi plates at 16°C until the young adult stage. The young adult worms were transferred onto RNAi

plates containing 0.1g/ml FUDR to prevent the growth of progeny and shifted to 22°C. The adult population was scored every day or every other day. Animals that failed to respond to a gentle prodding with a platinum wire were scored as dead. Day 0 of adult lifespan is the day that the adult worms were exposed to FUDR. Statistical analysis was performed with the Kaplan-Meier method to test the null hypothesis (SPSS v.11). The lifespan assays were repeated two times and similar results were observed in both experiments.

Immunoprecipitation and Western Blot

N2, *daf-16::gfp*, *daf-2(e1370); daf-16::gfp*, or *Psod-3::gfp* mixed staged worms were collected by washing with M9 buffer, packed by centrifugation at 3000g for 30 sec and frozen in liquid nitrogen in ~100 μl aliquot. *Psod-3::gfp* worms were starved for 1 day to induce the GFP expression at a comparable level before collected. *daf-2(e1370); daf-16::gfp* worms were shifted to 25°C for 6 hrs before collected to induce nuclear localization of DAF-16::GFP. Depending on the size of the frozen worm pellet, approximately 4X volume of lysis buffer (50 mM HEPES pH 7.5, 1 mM EDTA, 150 mM NaCl, 10% Glycerol, 0.1% Triton X-100, 1 mM sodium fluoride and protease inhibitor cocktail) was added. The worm pellets were allowed to thaw at room temperature completely and then frozen in liquid nitrogen again. The thaw-and-freeze procedures were repeated four times. The worm lysate was then sonicated using Markson Ultrasonic Processor for 10 × 15 sec bursts with 30 sec pauses at the output of 60. The debris was removed by centrifugation. The worm lysate was subsequently pre-cleared with 1/20 volume of protein A slurry (Pierce) over night at 4°C. The pre-cleared lysate was incubated with antibody (10 μl antibody per 400 μg total protein) for 1.5 hr at 4°C. 1/10 volume of BSA-blocked protein A slurry was then added and incubated for 1.5 hr at 4°C. The protein A beads were then washed with lysis buffer for six times and the bound proteins were eluted by boiling in 2X sample buffer for 5 min. The anti-FTT-2 and anti-PAR-5 antibodies used for immunoprecipitation are kind gifts from Dr. Andy Golden (NIDDK, National Institutes of Health, Bethesda, MD). The anti-FTT-2 antibody was generated against a small peptide at the extreme C-terminus of FTT-2 (CAATDDTDANETEGGN), and the anti-PAR-5 antibody has been previously reported (Morton et al., 2002). Protein samples eluted from the protein A beads were separated on a 10% SDS gel and transferred onto nitrocellulose membrane (BA85 Protran® BioScience) followed by standard Western blot procedure. The primary antibodies used: anti-ACTIN (mouse, Chemicon International), anti-GFP (goat, Rockland), anti-FTT-2 (rabbit, a gift from Dr. Andy Golden) and anti-PAR-5 (rabbit, a gift from Dr. Andy Golden). The secondary antibodies are: anti-goat (Rockland), anti-mouse (Santa Cruz) and anti-rabbit (Rockland). The immunoprecipitation experiments were repeated three times.

Real-time PCR

Synchronized young adult worms of the indicated genotypes were grown at 16°C and collected by washing with M9 buffer and frozen in liquid nitrogen. Total RNA of ~100 μl worm pellet was isolated using the RNeasy® Mini Kit (Qiagen) and quality control was done by both gel electrophoresis and UV absorbance measurement. cDNAs were synthesized with random hexamers by using SuperScript™ III First-Strand Kit (Invitrogen) according to the manufacturer's protocol. Real-time PCR reactions were performed in a 20 μl volume using iQ™ SYBR® Green Supermix (BIO-RAD) in a 96-well plate. Duplicates for each sample were included for one single reaction. The real-time PCR primers for *act-1* are: Forward primer: 5′-CCAGGAATTGCTGATCGTATGCAGAA –3′; Reverse primer: 5′-TGGAGAGGGAAGCGAGGATAGA –3′ (product length: 133 bp). Primers for *sod-3* are: Forward primer: 5′-TCGCACTGCTTCAAAGCTTGTTCAA –3′; Reverse primer: 5′-CCAAATCTGCATAGTCAGATGGGAGAT –3′ (product length: 98 bp). Primers for *ftt-2*: Forward primer: 5′-TCGACAAGTTCCTCATTCCA -3′; Reverse primer: 5′-TAGCTTTGCTGCGACTTCTC -3′ (product length: 145 bp). Primers for *par-5*: Forward primer: 5′-AAGTCCCAGAAGGCTTACCA -3′; Reverse primer: 5′-

TGGCTGCATCTTGTCCTTAG -3′ (product length: 57 bp). Primers for C24B9.9: Forward primer: 5′-AAAAAGCCATGTTCCCGAAT -3′; Reverse primer5′-GCTGCGAAAAGCAAGAAAAT -3′ (product length: 137 bp). Primers for F53C3.12: Forward primer5′-CGTGTACAGAGACCCCGAAT -3′; Reverse primer: 5′-TGAAGTGCCACGTATTTGGA -3′ (product length: 92 bp). *act-1* was used as the internal control and the RNA level of a gene of interest was normalized to the *act-1* level for comparison. PCR reaction was initiated at 95°C for 10 minutes for denaturation followed by a 40-cycles consisting of 15 sec at 95°C and 60 sec at 60°C. The real-time PCR experiments were repeated three to four times using independent RNAi worms and RNA preparations. Dauer worms grown at 22°C were not used for RT-PCR experiments because the asynchrony among the different RNAi worms caused large variations in mRNA expression.

Brood size assay

The brood size of RNAi treated worms was determined at 22°C. For each RNAi, ~10 N2 L4 larvae worms were singled onto each RNAi plate and allowed to lay egg over night and then transferred to fresh RNAi plate each subsequent days to lay egg until reproduction ended. The total number of eggs laid and hatched on each plate was counted every day. The brood size assays were repeated two times.

Developmental rate assay

The developmental rate of each RNAi worm population was determined at 22°C. For each RNAi, six gravid adults were allowed to lay egg for 1 hr. The times required for the progeny to reach adulthood were scored. The developmental rate assays were repeated two times.

Results and Discussions

RNAi inactivation of *ftt-2*, but not *par-5*, enhances dauer formation

To identify new components of the *daf-2*/insulin-like signaling pathway, we used feeding RNAi to knock down a select group of molecules annotated as being involved in signal transduction (Rual et al., 2004) and specifically examined their potential role in *C. elegans* dauer formation. In general, feeding RNAi gene knock down is not an efficient way to reveal a possible dauer phenotype, probably because feeding RNAi does not work well in the nervous systems (Tavernarakis et al., 2000;Timmons et al., 2001). Interestingly, at the semi-restrictive temperature 22°C, the *daf-2(e1370)* mutant worms form 100% dauer for ~72 hr and then exit dauer to develop into gravid/sterile adults. This represents a sensitized genetic background for using feeding RNAi to identify new players in *daf-2*-mediated dauer regulation. We found that RNAi knock down of the two 14-3-3 encoding genes, *ftt-2* and *par-5*, greatly enhanced the dauer arrest phenotype of *daf-2(e1370)*. At 22°C, 100% of the *daf-2(e1370)* worms fed with *ftt-2* RNAi and 45% of the *daf-2(e1370)* worms fed with *par-5* RNAi remained as dauer at the 96 hr time point, whereas only 4.5% of the *daf-2(e1370)* worms fed with the empty vector control L4440 RNAi remained as dauer at this time point.

ftt-2 and *par-5* are the two putative 14-3-3 encoding genes in *C. elegans*. The predicted transcripts of these two genes share ~78.2% sequence identity at the nucleotide level and ~85.9% sequence identity at the amino acid level (Wang and Shakes, 1997). The *ftt-2* and *par-5* RNAi constructs we initially used for the dauer screen include the full-length sequence of *ftt-2* and *par-5* respectively. Stretches of consecutive identical sequence as long as 19 base pairs (bp) are detected between the *ftt-2* and *par-5* RNAi constructs and we suspected that these two RNAi constructs might cross-react and caused the knock down of both *ftt-2* and *par-5*. In order to evaluate the specific roles of *ftt-2* and *par-5* in dauer formation, we generated gene-specific RNAi constructs that targeted unique fragments corresponding to the 3′ coding and UTR regions of either *ftt-2* or *par-5* (Morton et al., 2002). Sequence alignment indicates that

the longest stretch of sequence identity between the gene-specific *ftt-2* and *par-5* RNAi constructs is only 6 bp. To verify the specificity of the RNAi constructs, we used reverse-transcription real-time PCR (RT-PCR) to quantify the *ftt-2* and *par-5* mRNA levels in wild type (N2) and *daf-2(e1370)* animals that were undergoing RNAi against either the *ftt-2* or *par-5* gene (Fig. 1A and 1B). We detected a specific 2-fold knock down of the *ftt-2* and *par-5* mRNA levels in worms exposed to the corresponding gene-specific RNAi. Furthermore, N2 worms fed with the *par-5*-specific RNAi bacteria for two generations showed severe embryonic lethality (data not shown), similar to that reported previously (Morton et al., 2002). In contrast, N2 worms treated with the *ftt-2* specific RNAi for two generations exhibited reduced brood size but did not show noticeable embryonic lethality (Fig. 4). The molecular and phenotypic evidence strongly supports that the *ftt-2* and *par-5* RNAi constructs we generated specifically targeted the corresponding genes.

We also used anti-FTT-2 and anti-PAR-5 immunoblotting to confirm that the FTT-2 and PAR-5 protein levels were reduced in the *daf-2(e1370)* dauer worms treated with the gene-specific RNAi at 22°C (Fig. 1D). We found that the anti-FTT-2 signal was specifically reduced in *daf-2(e1370)* worms treated with the *ftt-2* RNAi, but not in worms treated with the *par-5* RNAi. In contrast, we noticed that the anti-PAR-5 signal was reduced in worms treated with either the *par-5* or *ftt-2* RNAi. Similar results were also observed in N2 worms (Fig. 1C). Taken together the immunoblotting, the RT-PCR, and the phenotypic results, we propose that the anti-FTT-2 antibody specifically recognizes FTT-2, whereas the anti-PAR-5 antibody may cross-react with both PAR-5 and FTT-2.

We retested whether specific knock downs of either *par-5* or *ftt-2* were able to enhance the dauer arrest phenotype of *daf-2(e1370)* at 22°C. *daf-2(e1370)* worms were exposed to *par-5* or *ftt-2* RNAi starting as embryos and allowed to develop at 22°C. The empty vector L4440 was used as a negative control, and the *daf-2* RNAi was included as a positive control. At 96 hr, when most of the worms treated with L4440 RNAi exited dauer and developed into sterile/gravid adults, the majority of the *ftt-2* RNAi worms remained in the dauer stage (Table 1). In fact, the *ftt-2* RNAi treated *daf-2(e1370)* worms remained arrested as dauer for the entire length of our experiments, which were usually carried out for ~240 hr, similar to that of the positive control *daf-2* RNAi worms. In contrast, worms treated with *par-5* RNAi behaved similarly to worms treated with L4440 RNAi (Table 1). These results indicate that despite the high sequence homology between *par-5* and *ftt-2*, *ftt-2* has the unique function of interacting with the *daf-2* pathway and affecting dauer formation.

RNAi knock down of *ftt-2* in wild-type N2 or *rrf-3(pk1426)*, a strain that specifically enhances somatic RNAi effects (Simmer et al., 2002), background resulted in normal development and no observable dauer arrest phenotype at either 22°C or 25°C (Table 1 and data not shown). This is not surprising as RNAi inactivation of *daf-2* did not induce dauer formation in the N2 background (Table 1). Moreover, our RT-PCR and immunoblotting experiments indicate that the gene-specific *ftt-2* RNAi only causes a ~2-fold decrease in FTT-2 levels (Fig. 1). It is possible that such a modest reduction in FTT-2, while sufficient to promote dauer arrest in a sensitized background, is not able to signal dauer arrest in a wild-type background. Although a *ftt-2* deletion mutant is available through the knockout consortium (http://www.wormbase.org/), we are not able to analyze its dauer formation phenotype because the homozygous *ftt-2* deletion mutant is not viable (JL & SSL, unpublished data; Wang et al., 2006).

RNAi inactivation of *ftt-2* promotes DAF-16::GFP nuclear localization

Our results indicate that reduced *ftt-2* expression specifically enhances the dauer formation phenotype associated with reduced *daf-2*/insulin-like signaling. Because *daf-16* is the major downstream effecter of *daf-2* signaling and increased DAF-16 activity is critical for promoting

dauer arrest, we investigated whether RNAi knock down of *ftt-2* might affect *daf-16* activity. A key step of DAF-16 regulation is the translocation of DAF-16 from the cytoplasm to the nucleus. We used feeding RNAi to inactivate *ftt-2* in worms carrying an integrated *gfp*-fused *daf-16* transgene (*daf-16::gfp*) (Lee et al., 2001). The *daf-16::gfp* worms fed with *ftt-2* RNAi tended to arrest at the L3 stage, but they developed to the L3 stage at a rate similar to that of control RNAi worms. We therefore monitored the DAF-16::GFP localization in L3 animals. When the *daf-16::gfp* worms were fed with the control L4440 RNAi, the DAF-16::GFP fusion protein was evenly distributed in the cytoplasm and nucleus of cells throughout the body of the worm (Fig. 2A). Consistent with previous reports, when *daf-2* was inactivated by RNAi, the DAF-16::GFP fusion protein became intensely localized in the nucleus of cells, although some cytoplasmic staining remained detectable (Fig. 2D) (Lin et al., 2001). Interestingly, when *ftt-2* was RNAi inactivated, the DAF-16::GFP fusion protein was also dramatically enriched in the nucleus of cells (Fig. 2B), with a low level of cytoplasmic DAF-16::GFP remained detectable. In contrast, *par-5* RNAi knock down did not significantly affect the localization pattern of DAF-16::GFP (Fig. 2C). These results indicate that reduced *ftt-2* expression specifically induces the nuclear enrichment of DAF-16.

Enhanced DAF-16 transcriptional activities upon *ftt-2* RNAi

Because nuclear translocation of DAF-16 may allow DAF-16 to access its transcriptional targets, we next investigated whether *ftt-2* RNAi promoted the transcriptional activities of DAF-16. To accomplish this, we exposed N2 or *daf-16(mgDf47)* null mutant worms to *ftt-2* RNAi and monitored the mRNA levels of *sod-3*, a well-characterized DAF-16 direct target gene (Honda and Honda, 1999;Wook Oh et al., 2006). Consistent with previous reports (Honda and Honda, 1999), we detected ~5-fold up-regulation of *sod-3* levels in N2 worms treated with *daf-2* RNAi (Fig. 3A). Importantly, when N2 worms were fed *ftt-2* RNAi, the expression levels of *sod-3* were upregulated about 2-fold (Fig. 3A), suggesting that the transcriptional activities of DAF-16 were elevated. The increased *sod-3* expression in *ftt-2* RNAi treated N2 worms was not due to a change in *daf-16* levels, as the *daf-16* mRNA levels were not significantly different in worms treated with the different RNAi (data not shown). Consistent with the distinction between *ftt-2* and *par-5* on dauer promotion and DAF-16::GFP translocation, reduction of *par-5* did not affect DAF-16 transcriptional activities. Similar RNAi experiments performed in the *daf-16(mgDf47)* null mutant indicate that the induction of *sod-3* expression observed in the *ftt-2* or *daf-2* RNAi worms was mediated by *daf-16*. In *daf-16(mgDf47)* null mutant worms treated with control L4440 RNAi, very low basal expression of *sod-3* was observed (Fig. 3A). Furthermore, in *daf-16(mgDf47)* null mutant worms, neither *ftt-2* nor *daf-2* RNAi had any significant effect on the low basal level of *sod-3* expression (Fig. 3A).

We examined the mRNA levels of additional DAF-16 downstream genes (Murphy et al., 2003). As expected, the DAF-16 activated genes C24B9.9 & F53C3.12 exhibited robust expression changes when worms were treated with *daf-2* RNAi *vs. daf-16* RNAi (Fig. 3B & 3C). For these two genes, increased expression was also detected in *ftt-2* RNAi worms, consistent with an elevation of DAF-16 activities in *ftt-2* knock down worms. The results we described thus far suggest the model that RNAi inactivation of *ftt-2* induces the nuclear translocation of DAF-16 and promotes the transcription of some DAF-16 downstream genes.

RNAi inactivation of *ftt-2* leads to shortened lifespan

Because reduced *daf-2* signaling and increased *daf-16* activities are often associated with enhanced dauer formation and extended adult lifespan, we investigated whether RNAi inactivation of *ftt-2* in worms also affected adult lifespan. We found that the *ftt-2* RNAi knock down worms had a much shorter adult lifespan compared to the control RNAi worms (Table 2). In contrast, the *par-5* RNAi knock down worms exhibited normal lifespan (Table 2). Interestingly, *ftt-2* RNAi did not appear to affect the extended lifespan phenotype of *daf-2*

(e1370) worms (Table 2). Moreover, we determined that the *ftt-2* RNAi treated worms developed into adults at a normal rate (*control RNAi: 46.5 +/− 2.5 hr, N= 717; ftt-2 RNAi: 44.2 +/− 2.2 hr, N=186*) and exhibited no obvious developmental defects. Taken together, the results indicate that *ftt-2* RNAi leads to a reduced lifespan in wild-type background, but *ftt-2* RNAi does not appear to shorten lifespan by causing non-specific sickness in worms (Berdichevsky et al., 2006;Wang et al., 2006). The lifespan shortening effect of *ftt-2* RNAi knock down was somewhat unexpected based on our observation that *ftt-2* RNAi promoted dauer formation of *daf-2(e1370)* worms. On the other hand, the lifespan and dauer phenotypes associated with the *daf-2*/insulin-like signaling pathway have been shown to be mediated by distinct effecter complexes. For instance, the *eak* mutations robustly enhance the dauer formation phenotype associated with the *akt-1* mutant (the serine/threonine kinase downstream of *daf-2*) but have little effect on the longevity of the *akt-1* mutant worms (Hu et al., 2006); the *smk-1* gene specifically interferes with the ability of *daf-16* to affect lifespan but has little effect on *daf-16*-mediated dauer regulation (Wolff et al., 2006). Furthermore, because 14-3-3 proteins are known to bind to a large number of substrates, FTT-2 is most certainly involved in numerous diverse functions. RNAi inactivation of *ftt-2* will likely disrupt multiple biological pathways that together may result in lifespan shortening. Two recent papers implicated 14-3-3 proteins in mediating the longevity promoting effect of SIR-2.1 by bridging the interactions of SIR-2.1 and DAF-16 in the nucleus upon stress signals (Berdichevsky et al., 2006;Wang et al., 2006). An interesting possibility is that, in the *ftt-2* knock down worms, although more cytoplasmic DAF-16 are released into the nucleus to turn on some DAF-16 downstream genes, such a beneficial effect may be countered by the dissociation of the nuclear 14-3-3/SIR-2.1/DAF-16 protein complexes and result in lifespan shortening.

FTT-2 forms a complex with DAF-16 *in vivo*

14-3-3 proteins usually function by binding to phosphorylated ligands (Fu et al., 2000). Recent studies in cultured mammalian cells indicate that the 14-3-3ζ isoform binds to phosphorylated FOXO3a, one of the DAF-16 mammalian homologs, and sequesters FOXO3a in the cytoplasm (Brunet et al., 1999). Furthermore, *in vitro* pull-down assays show that the mammalian 14-3-3ζ isoform is able to bind to phosphorylated DAF-16 (Cahill et al., 2001). Therefore, it is possible that FTT-2 forms a complex with DAF-16 in *C. elegans*. We used co-immunoprecipitation (co-IP) experiments to test this possibility. Because we do not have an antibody that could detect endogenous DAF-16 robustly, we used worm extracts from the *daf-16::gfp* strains and an anti-FTT-2 antibody for immunoprecipitation. The co-IP experiments showed that when FTT-2 was specifically immunoprecipitated, DAF-16::GFP was also recovered (Fig. 5A). In the same experiment, a GFP protein driven by the *sod-3* promoter (*Psod-3::gfp*) was not co-immunoprecipitated with FTT-2, indicating that FTT-2 and DAF-16::GFP forms a specific complex in worms. Furthermore, co-IP experiments carried out using worm extracts from animals treated with *ftt-2* RNAi showed that a much reduced level of FTT-2 was immunoprecipitated and consequently no detectable DAF-16::GFP was co-immunoprecipitated (Fig. 5B). We also carried out co-IP experiments using *daf-2(e1370); daf-16::gfp* worms that were cultured at the non-permissive temperature for six hours. Under this condition, the majority of DAF-16::GFP was observed in the nuclei of cells, presumably due to the inactivation of DAF-2 at 25°C. We found that reduced levels of DAF-16::GFP was co-immunoprecipitated with FTT-2 in *daf-2(e1370); daf-16::gfp* worm extracts compared to that of *daf-16::gfp*, even though similar levels of FTT-2 was immunoprecipitated in both extracts (Fig. 5A). These results are consistent with the model that when *daf-2*/insulin-like signaling is inactivated, DAF-16 becomes dephosphorylated and dissociates from 14-3-3 binding.

Our co-IP results together with the previously published *in vitro* pull-down evidence (Cahill et al., 2001) suggest that FTT-2 likely directly binds to phosphorylated DAF-16 in *C.*

elegans. Because 14-3-3 proteins are abundantly distributed in the cytoplasm, the binding of FTT-2 with DAF-16 may sequester DAF-16 in the cytoplasm. We hypothesize that when *ftt-2* is depleted by RNAi, DAF-16 is free to move into the nucleus and execute its transcriptional role.

In our co-IP experiments, a low level of DAF-16::GFP also co-immunoprecipitated with PAR-5 when anti-PAR-5 was used for immunoprecipitation. The FTT-2 and PAR-5 antibodies we used were generated against two distinct FTT-2 and PAR-5 peptides (kind gifts from Dr. Golden). However, as described earlier, in immunoblotting experiments, we found that whereas the anti-FTT-2 antibody appears to be highly specific, the anti-PAR-5 antibody may cross-react with the FTT-2 protein (Fig. 1). Therefore, the weak binding we detected between PAR-5 and DAF-16::GFP may be due to cross-reactivity of the anti-PAR-5 antibody to FTT-2. Alternatively, PAR-5 may indeed form a complex with DAF-16::GFP in worms. Because our experiments indicate that PAR-5 does not affect *daf-2*-mediated dauer formation, DAF-16 subcellular localization or DAF-16 transcriptional activities, PAR-5 may be involved in other aspects of DAF-16 functions (Berdichevsky et al., 2006).

Our analyses demonstrate that specific knock down of *ftt-2*, but not *par-5*, affects dauer formation, DAF-16 localization, and DAF-16 transcriptional activities. Such specificity is consistent with the expression patterns of FTT-2 and PAR-5. Using northern blotting analyses, *par-5* is detected to express highly in the embryos and its mRNA level drops drastically by the L1 stage and remains low through larval development. *ftt-2* is also found to be the most highly expressed in embryos but its expression through larval stages only drops a little compared to that in embryos (Wang and Shakes, 1997). Also, whereas *par-5* expression is highly germline enriched, *ftt-2* is not (Wang and Shakes, 1997). Using GFP fusion strategies, PAR-5::GFP is shown to express strongly in the neurons and the intestine of transgenic larvae and FTT-2::GFP is shown to express most strongly in the pharynx and the nervous system, and weakly in the intestine of transgenic larvae (Wang et al., 2006). Based on the expression patterns of FTT-2 and PAR-5, it is not surprising that FTT-2 has important functions during *C. elegans* larval development. Furthermore, as FTT-2 and PAR-5 express in overlapping but distinct tissues, it is also expected that they will have different functions. Interestingly, in our RT-PCR experiments (Fig. 1), we noticed that specific knock down of *par-5* led to ~2-fold increase in *ftt-2* mRNA expression, probably due to a yet unknown compensation mechanism. Our results indicate that *C. elegans* has assigned different tasks for the closely related members of the 14-3-3 family, further supporting the notion that 14-3-3 proteins have isoform-specific functions (Roberts and de Bruxelles, 2002).

In summary, we report here that the 14-3-3 protein FTT-2 specifically regulates dauer formation, DAF-16 subcellular localization, and DAF-16 transcriptional activities in *C. elegans*. We provide evidence that FTT-2 forms a complex with DAF-16 in worm, similar to that in mammalian cultured cells. The complex formation between FTT-2 and DAF-16 likely results in cytoplasmic sequestration of DAF-16 and prevents it from regulating its transcriptional targets. Our results advance the understanding of the regulation of DAF-16, an important determinant of longevity, metabolism, and development, and further highlight the high degree of conservation between the *C. elegans daf-2* and the mammalian insulin/IGF-1 signal transduction pathways.

Acknowledgements

We thank members of the Lee, Liu, and Kemphues labs (Cornell University, Ithaca NY) for helpful discussion. We especially thank Dr. Diane Morton (Cornell University, Ithaca NY) for providing the PCR primers for *ftt-2* and *par-5*, and for insightful discussion. We thank the Lis lab (Cornell University, Ithaca NY) for usage of the real-time PCR machine and we are grateful to Behfar Ardehali for technical assistance. We are especially grateful to Dr. Andy Golden (NIDDK, National Institutes of Health, Bethesda, MD) for providing the anti-FTT-2 and anti-PAR-5 antibodies. We thank Philippe Vaglio for assistance with the bioinformatics. We also thank CGC for providing strains.

The RNAi resource used here was supported by a NCI grant to MV. This work was supported by a New Scholar Award in Aging from the Ellison Medical Foundation and a R01 grant AG024425-01 from the NIA awarded to SSL.

References

Agarwal-Mawal A, Qureshi HY, Cafferty PW, Yuan Z, Han D, Lin R, Paudel HK. 14-3-3 connects glycogen synthase kinase-3 beta to tau within a brain microtubule-associated tau phosphorylation complex. J Biol Chem 2003;278:12722–8. [PubMed: 12551948]

Berdichevsky A, Viswanathan M, Horvitz HR, Guarente L. C. elegans SIR-2.1 interacts with 14-3-3 proteins to activate DAF-16 and extend life span. Cell 2006;125:1165–77. [PubMed: 16777605]

Birkenkamp KU, Coffer PJ. Regulation of cell survival and proliferation by the FOXO (Forkhead box, class O) subfamily of Forkhead transcription factors. Biochem Soc Trans 2003;31:292–7. [PubMed: 12546704]

Brunet A, Bonni A, Zigmond MJ, Lin MZ, Juo P, Hu LS, Anderson MJ, Arden KC, Blenis J, Greenberg ME. Akt promotes cell survival by phosphorylating and inhibiting a Forkhead transcription factor. Cell 1999;96:857–68. [PubMed: 10102273]

Cahill CM, Tzivion G, Nasrin N, Ogg S, Dore J, Ruvkun G, Alexander-Bridges M. Phosphatidylinositol 3-kinase signaling inhibits DAF-16 DNA binding and function via 14-3-3-dependent and 14-3-3-independent pathways. J Biol Chem 2001;276:13402–10. [PubMed: 11124266]

Chen MS, Ryan CE, Piwnica-Worms H. Chk1 kinase negatively regulates mitotic function of Cdc25A phosphatase through 14-3-3 binding. Mol Cell Biol 2003;23:7488–97. [PubMed: 14559997]

Clancy DJ, Gems D, Harshman LG, Oldham S, Stocker H, Hafen E, Leevers SJ, Partridge L. Extension of life-span by loss of CHICO, a Drosophila insulin receptor substrate protein. Science 2001;292:104–6. [PubMed: 11292874]

Datta SR, Katsov A, Hu L, Petros A, Fesik SW, Yaffe MB, Greenberg ME. 14-3-3 proteins and survival kinases cooperate to inactivate BAD by BH3 domain phosphorylation. Mol Cell 2000;6:41–51. [PubMed: 10949026]

DeLille JM, Sehnke PC, Ferl RJ. The arabidopsis 14-3-3 family of signaling regulators. Plant Physiol 2001;126:35–8. [PubMed: 11351068]

Forrest A, Gabrielli B. Cdc25B activity is regulated by 14-3-3. Oncogene 2001;20:4393–401. [PubMed: 11466620]

Fu H, Subramanian RR, Masters SC. 14-3-3 proteins: structure, function, and regulation. Annu Rev Pharmacol Toxicol 2000;40:617–47. [PubMed: 10836149]

Fu H, Xia K, Pallas DC, Cui C, Conroy K, Narsimhan RP, Mamon H, Collier RJ, Roberts TM. Interaction of the protein kinase Raf-1 with 14-3-3 proteins. Science 1994;266:126–9. [PubMed: 7939632]

Gems D, Sutton AJ, Sundermeyer ML, Albert PS, King KV, Edgley ML, Larsen PL, Riddle DL. Two pleiotropic classes of daf-2 mutation affect larval arrest, adult behavior, reproduction and longevity in Caenorhabditis elegans. Genetics 1998;150:129–55. [PubMed: 9725835]

Gottlieb S, Ruvkun G. daf-2, daf-16 and daf-23: genetically interacting genes controlling Dauer formation in Caenorhabditis elegans. Genetics 1994;137:107–20. [PubMed: 8056303]

Grozinger CM, Schreiber SL. Regulation of histone deacetylase 4 and 5 and transcriptional activity by 14-3-3-dependent cellular localization. Proc Natl Acad Sci U S A 2000;97:7835–40. [PubMed: 10869435]

Halaschek-Wiener J, Khattra JS, McKay S, Pouzyrev A, Stott JM, Yang GS, Holt RA, Jones SJ, Marra MA, Brooks-Wilson AR, Riddle DL. Analysis of long-lived C. elegans daf-2 mutants using serial analysis of gene expression. Genome Res 2005;15:603–15. [PubMed: 15837805]

Holzenberger M, Dupont J, Ducos B, Leneuve P, Geloen A, Even PC, Cervera P, Le Bouc Y. IGF-1 receptor regulates lifespan and resistance to oxidative stress in mice. Nature 2003;421:182–7. [PubMed: 12483226]

Honda Y, Honda S. The daf-2 gene network for longevity regulates oxidative stress resistance and Mn-superoxide dismutase gene expression in Caenorhabditis elegans. Faseb J 1999;13:1385–93. [PubMed: 10428762]

Hu PJ, Xu J, Ruvkun G. Two membrane-associated tyrosine phosphatase homologs potentiate C. elegans AKT-1/PKB signaling. PLoS Genet 2006;2:e99. [PubMed: 16839187]

Ichimura T, Isobe T, Okuyama T, Takahashi N, Araki K, Kuwano R, Takahashi Y. Molecular cloning of cDNA coding for brain-specific 14-3-3 protein, a protein kinase-dependent activator of tyrosine and tryptophan hydroxylases. Proc Natl Acad Sci U S A 1988;85:7084–8. [PubMed: 2902623]

Irie K, Gotoh Y, Yashar BM, Errede B, Nishida E, Matsumoto K. Stimulatory effects of yeast and mammalian 14-3-3 proteins on the Raf protein kinase. Science 1994;265:1716–9. [PubMed: 8085159]

Jones DH, Ley S, Aitken A. Isoforms of 14-3-3 protein can form homo- and heterodimers in vivo and in vitro: implications for function as adapter proteins. FEBS Lett 1995;368:55–8. [PubMed: 7615088]

Kenyon C, Chang J, Gensch E, Rudner A, Tabtiang R. A C. elegans mutant that lives twice as long as wild type. Nature 1993;366:461–4. [PubMed: 8247153]

Kimura KD, Tissenbaum HA, Liu Y, Ruvkun G. daf-2, an insulin receptor-like gene that regulates longevity and diapause in Caenorhabditis elegans. Science 1997;277:942–6. [PubMed: 9252323]

Larsen PL, Albert PS, Riddle DL. Genes that regulate both development and longevity in Caenorhabditis elegans. Genetics 1995;139:1567–83. [PubMed: 7789761]

Lee RY, Hench J, Ruvkun G. Regulation of C. elegans DAF-16 and its human ortholog FKHRL1 by the daf-2 insulin-like signaling pathway. Curr Biol 2001;11:1950–7. [PubMed: 11747821]

Lee SS, Kennedy S, Tolonen AC, Ruvkun G. DAF-16 target genes that control C. elegans life-span and metabolism. Science 2003a;300:644–7. [PubMed: 12690206]

Lee SS, Lee RY, Fraser AG, Kamath RS, Ahringer J, Ruvkun G. A systematic RNAi screen identifies a critical role for mitochondria in C. elegans longevity. Nat Genet 2003b;33:40–8. [PubMed: 12447374]

Lin K, Dorman JB, Rodan A, Kenyon C. daf-16: An HNF-3/forkhead family member that can function to double the life-span of Caenorhabditis elegans. Science 1997;278:1319–22. [PubMed: 9360933]

Lin K, Hsin H, Libina N, Kenyon C. Regulation of the Caenorhabditis elegans longevity protein DAF-16 by insulin/IGF-1 and germline signaling. Nat Genet 2001;28:139–45. [PubMed: 11381260]

Martin H, Patel Y, Jones D, Howell S, Robinson K, Aitken A. Antibodies against the major brain isoforms of 14-3-3 protein. An antibody specific for the N-acetylated amino-terminus of a protein. FEBS Lett 1993;331:296–303. [PubMed: 8375512]

Masters SC, Pederson KJ, Zhang L, Barbieri JT, Fu H. Interaction of 14-3-3 with a nonphosphorylated protein ligand, exoenzyme S of Pseudomonas aeruginosa. Biochemistry 1999;38:5216–21. [PubMed: 10213629]

McElwee J, Bubb K, Thomas JH. Transcriptional outputs of the Caenorhabditis elegans forkhead protein DAF-16. Aging Cell 2003;2:111–21. [PubMed: 12882324]

Morton DG, Shakes DC, Nugent S, Dichoso D, Wang W, Golden A, Kemphues KJ. The Caenorhabditis elegans par-5 gene encodes a 14-3-3 protein required for cellular asymmetry in the early embryo. Dev Biol 2002;241:47–58. [PubMed: 11784094]

Murphy CT, McCarroll SA, Bargmann CI, Fraser A, Kamath RS, Ahringer J, Li H, Kenyon C. Genes that act downstream of DAF-16 to influence the lifespan of Caenorhabditis elegans. Nature 2003;424:277–83. [PubMed: 12845331]

Obsil T, Ghirlando R, Klein DC, Ganguly S, Dyda F. Crystal structure of the 14-3-3zeta:serotonin N-acetyltransferase complex. a role for scaffolding in enzyme regulation. Cell 2001;105:257–67. [PubMed: 11336675]

Ogg S, Paradis S, Gottlieb S, Patterson GI, Lee L, Tissenbaum HA, Ruvkun G. The Fork head transcription factor DAF-16 transduces insulin-like metabolic and longevity signals in C. elegans. Nature 1997;389:994–9. [PubMed: 9353126]

Peng CY, Graves PR, Thoma RS, Wu Z, Shaw AS, Piwnica-Worms H. Mitotic and G2 checkpoint control: regulation of 14-3-3 protein binding by phosphorylation of Cdc25C on serine-216. Science 1997;277:1501–5. [PubMed: 9278512]

Pozuelo Rubio M, Geraghty KM, Wong BH, Wood NT, Campbell DG, Morrice N, Mackintosh C. 14-3-3-affinity purification of over 200 human phosphoproteins reveals new links to regulation of cellular metabolism, proliferation and trafficking. Biochem J 2004;379:395–408. [PubMed: 14744259]

Riddle, D-L.; Albert, P-S. Genetic and environmental regulation of Dauer larva development. In: Riddle, DL.; Blumenthal, T.; Meyer, BJ.; Priess, JR., editors. Cold Spring Harbor Monograph Series; C.

elegans II. 33. Cold Spring Harbor Laboratory Press {a}, 10 Skyline Drive; Plainview, New York 11803, USA: 1997. 1997. p. 739-768.

Riddle DL, Swanson MM, Albert PS. Interacting genes in nematode dauer larva formation. Nature 1981;290:668–71. [PubMed: 7219552]

Roberts MR, de Bruxelles GL. Plant 14-3-3 protein families: evidence for isoform-specific functions? Biochem Soc Trans 2002;30:373–8. [PubMed: 12196097]

Rual JF, Ceron J, Koreth J, Hao T, Nicot AS, Hirozane-Kishikawa T, Vandenhaute J, Orkin SH, Hill DE, van den Heuvel S, Vidal M. Toward improving Caenorhabditis elegans phenome mapping with an ORFeome-based RNAi library. Genome Res 2004;14:2162–8. [PubMed: 15489339]

Simmer F, Tijsterman M, Parrish S, Koushika SP, Nonet ML, Fire A, Ahringer J, Plasterk RH. Loss of the putative RNA-directed RNA polymerase RRF-3 makes C. elegans hypersensitive to RNAi. Curr Biol 2002;12:1317–9. [PubMed: 12176360]

Tatar M, Kopelman A, Epstein D, Tu MP, Yin CM, Garofalo RS. A mutant Drosophila insulin receptor homolog that extends life-span and impairs neuroendocrine function. Science 2001;292:107–10. [PubMed: 11292875]

Tavernarakis N, Wang SL, Dorovkov M, Ryazanov A, Driscoll M. Heritable and inducible genetic interference by double-stranded RNA encoded by transgenes. Nat Genet 2000;24:180–3. [PubMed: 10655066]

Timmons L, Court DL, Fire A. Ingestion of bacterially expressed dsRNAs can produce specific and potent genetic interference in Caenorhabditis elegans. Gene 2001;263:103–12. [PubMed: 11223248]

Wang W, Shakes DC. Molecular evolution of the 14-3-3 protein family. J Mol Evol 1996;43:384–98. [PubMed: 8798343]

Wang W, Shakes DC. Expression patterns and transcript processing of ftt-1 and ftt-2, two C. elegans 14-3-3 homologues. J Mol Biol 1997;268:619–30. [PubMed: 9171285]

Wang Y, Oh SW, Deplancke B, Luo J, Walhout AJ, Tissenbaum HA. C. elegans 14-3-3 proteins regulate life span and interact with SIR-2.1 and DAF-16/FOXO. Mech Ageing Dev 2006;127:741–7. [PubMed: 16860373]

Wolff S, Ma H, Burch D, Maciel GA, Hunter T, Dillin A. SMK-1, an essential regulator of DAF-16-mediated longevity. Cell 2006;124:1039–53. [PubMed: 16530049]

Wook Oh S, Mukhopadhyay A, Dixit BL, Raha T, Green MR, Tissenbaum HA. Identification of direct DAF-16 targets controlling longevity, metabolism and diapause by chromatin immunoprecipitation. Nat Genet 2006;38:251–7. [PubMed: 16380712]

Yaffe MB. How do 14-3-3 proteins work?-- Gatekeeper phosphorylation and the molecular anvil hypothesis. FEBS Lett 2002;513:53–7. [PubMed: 11911880]

Yaffe MB, Rittinger K, Volinia S, Caron PR, Aitken A, Leffers H, Gamblin SJ, Smerdon SJ, Cantley LC. The structural basis for 14-3-3:phosphopeptide binding specificity. Cell 1997;91:961–71. [PubMed: 9428519]

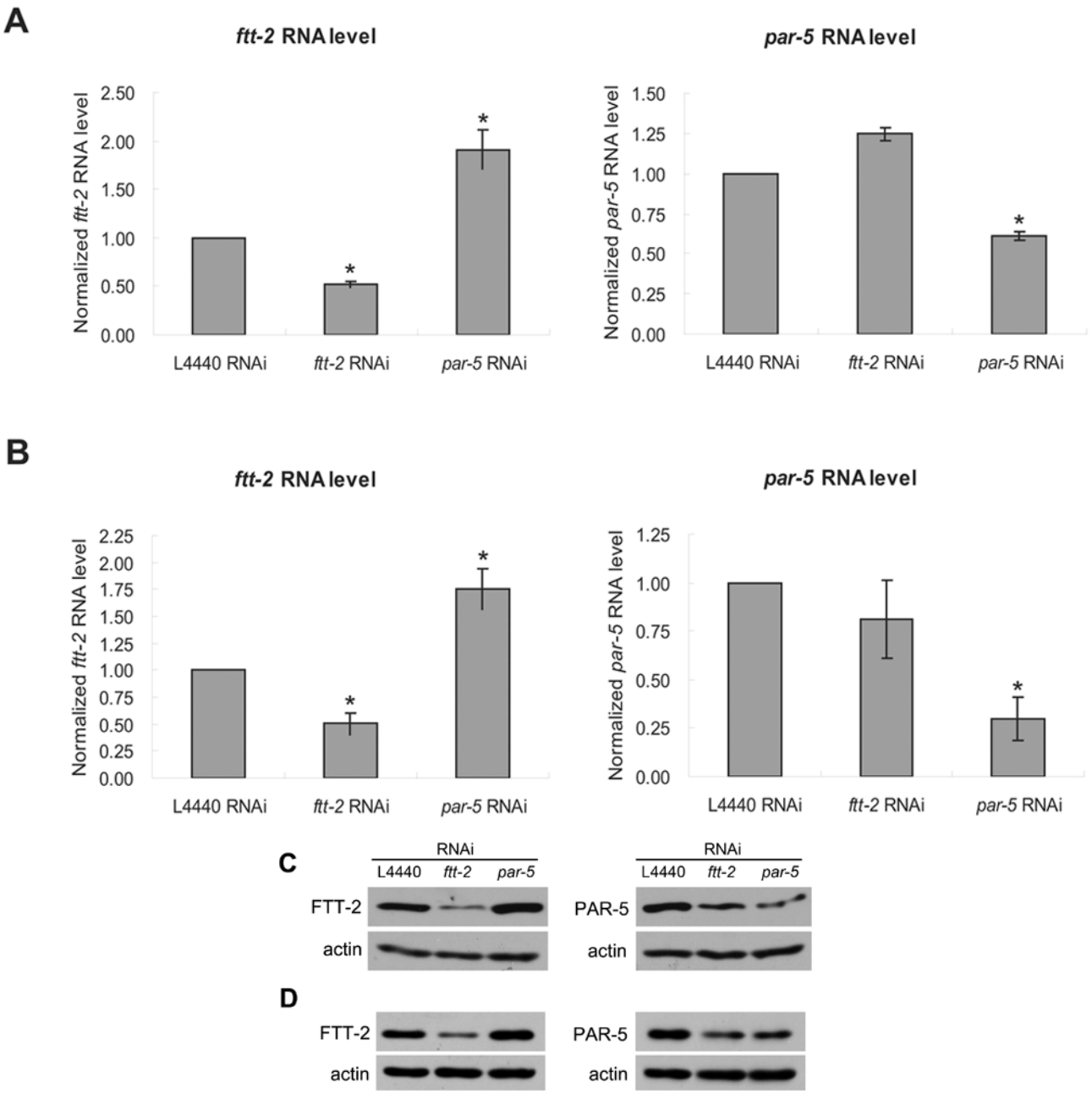

Figure 1.

The *ftt-2* and *par-5* RNAi constructs are gene-specific. N2 (A) or *daf-2(e1370)* (B) worms were exposed to feeding RNAi bacteria starting as L1 at 16°C. Total RNA was extracted from young adult RNAi worms for real-time-PCR analysis. The y-axis indicates the relative RNA levels normalized to the RNA expression levels of the internal control *act-1*. The relative RNA levels for worms treated with the L4440 control RNAi is set as 1. The average of four independent experiments is shown and the error bars represent standard error of the mean (SEM). P-value of <0.01 (*) was determined by Student's t-test. FTT-2 or PAR-5 immunoblotting was performed using young adult N2 worms exposed to the indicated RNAi bacteria at 16°C (C) or *daf-2(e1370)* dauer worms exposed to the indicated RNAi bacteria at 22°C (D).

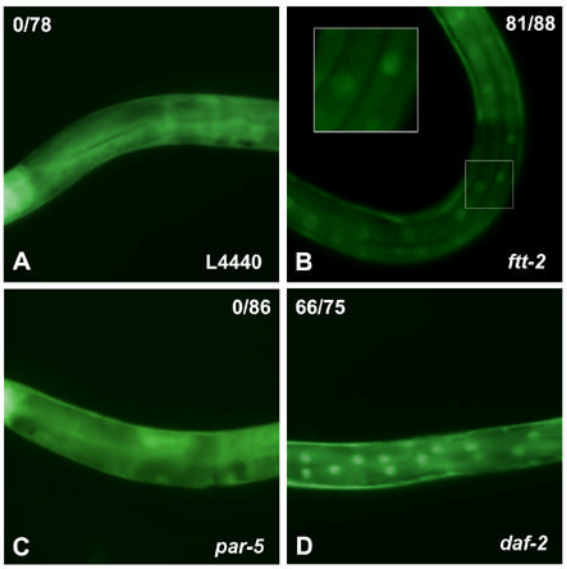

Figure 2.

ftt-2 RNAi, but not *par-5* RNAi, causes DAF-16::GFP accumulation in the nucleus. DAF-16::GFP worms were exposed to the various RNAi bacteria starting as embryos at 16° C. DAF-16::GFP expression of the RNAi worms at the L3 stage are shown. None of the 78 worms exposed to the control L4440 RNAi (panel A) nor the 86 worms exposed to *par-5* RNAi (panel C) showed DAF-16::GFP nuclear localization. In contrast, 81 out of 88 worms exposed to *ftt-2* RNAi (panel B) and 66 out of 75 exposed to *daf-2* RNAi (panel D) exhibited prominent DAF-16::GFP nuclear localization. A small number of *daf-2* RNAi or *ftt-2* RNAi worms continued to exhibit cytoplasmic DAF-16::GFP, probably due to variable RNAi efficiency. The images (A–D) were captured using identical magnification and exposure time.

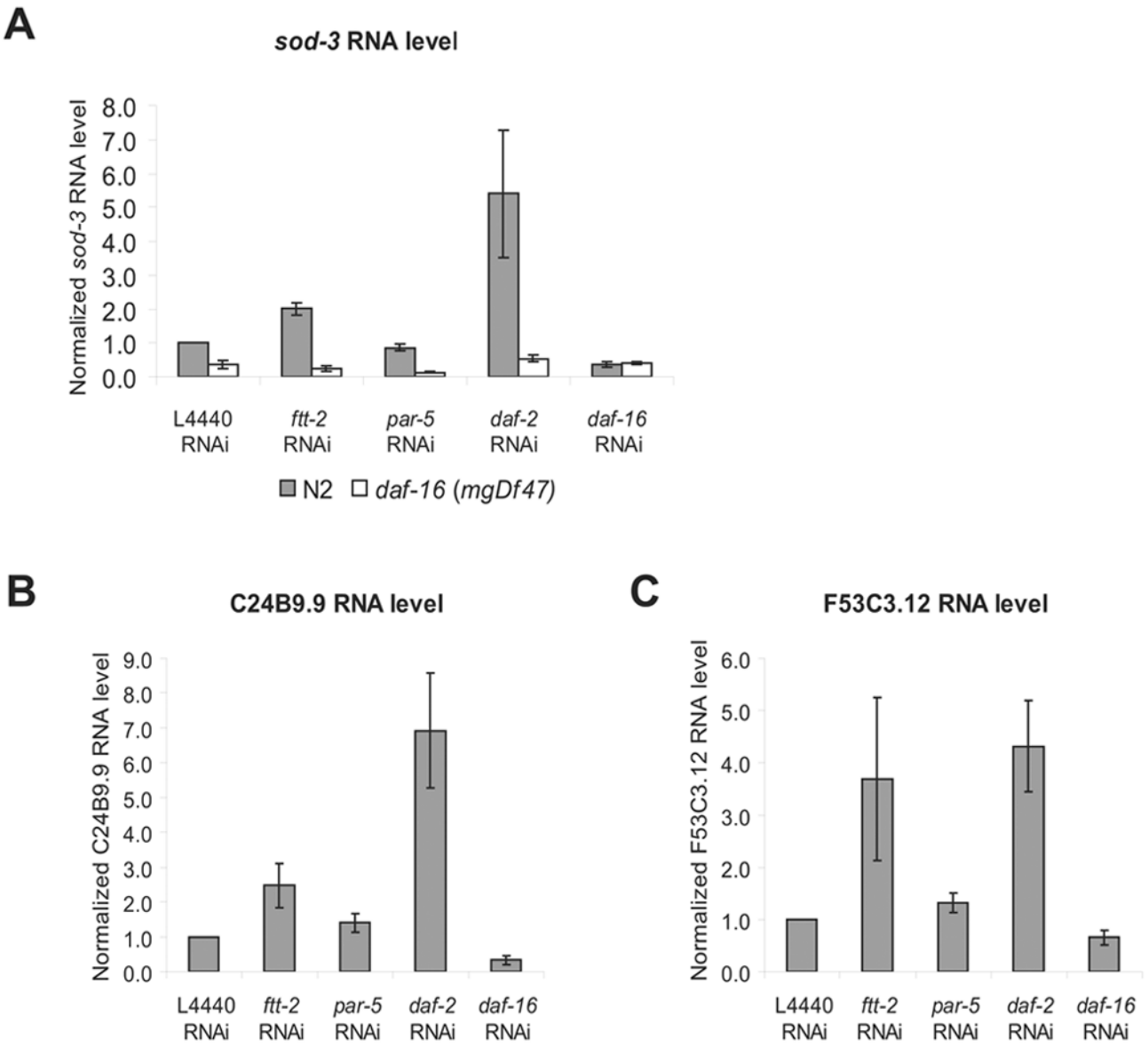

Figure 3.

RNAi inactivation of *ftt-2* results in the up-regulation of *daf-16*-dependent mRNA expression of *sod-3* (A), C24B9.9 (B) and F53C3.12 (C). N2 worms or *daf-16 (mgDf47)* null mutant worms were exposed to the indicated RNAi starting as L1 at 16°C. Total RNA was extracted from young adult RNAi worms for real-time-PCR analysis. The y-axis indicates the RNA levels normalized to the RNA expression levels of the internal control *act-1*. The relative RNA levels for N2 worms treated with the L4440 control RNAi is set as 1. The average of four independent experiments is shown and the error bars represent SEM.

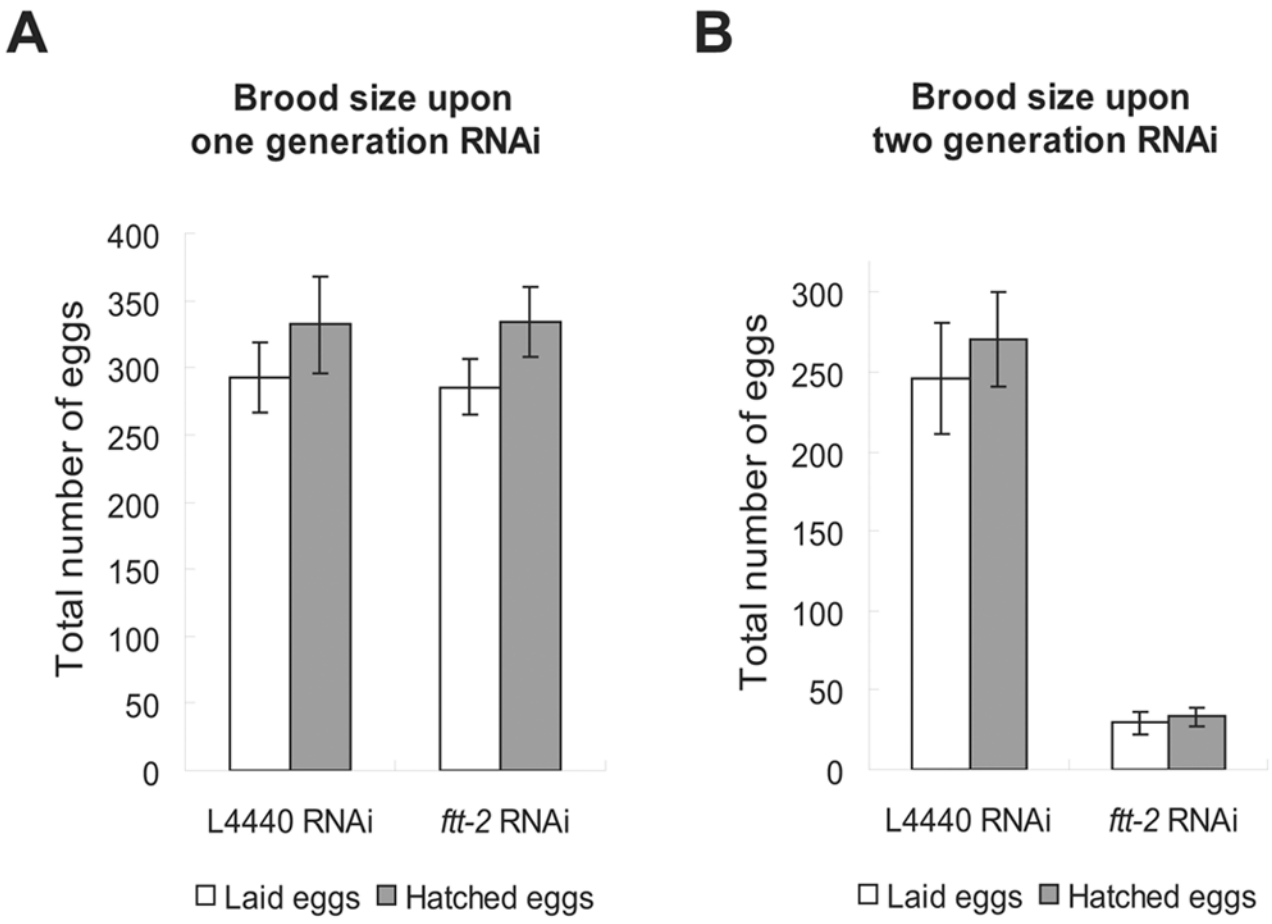

Figure 4.

The brood size of *ftt-2* RNAi worms upon one generation (A) or two generations (B) of RNAi treatment. The average brood size of ~10 worms for each RNAi treatment is shown. Error bars represent SEM.

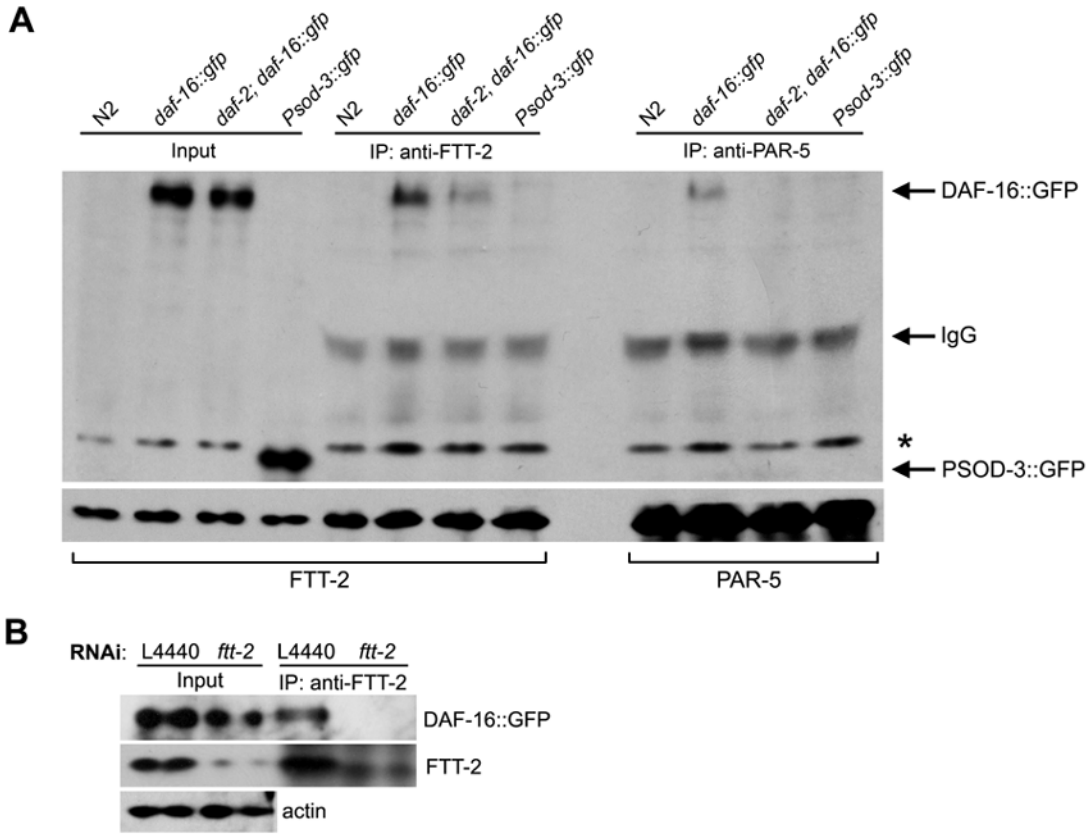

Figure 5.

FTT-2 forms a complex with DAF-16::GFP in *C. elegans*. (A) Worm extracts from mixed staged *daf-16::gfp* worms (*daf-16(mgDf47)*; xrls87[*daf-16a::gfp*::DAF-16B, *rol-6*(su1006)]) or *daf-2(e1370); daf-16::gfp* worms that had been incubated at 25°C for 6 hrs were immunoprecipitated with an anti-FTT-2 or an anit-PAR-5 antibody and the precipitated proteins were immunoblotted with an anti-GFP antibody (upper panel) and an anti-FTT-2 or an anti-PAR-5 antibody (lower panel). Extracts from N2 and *Psod-3::gfp* worms were used as negative controls. *: Non-specific band. (B) Worm extracts were prepared from *daf-16::gfp* L3 larvae treated with *ftt-2* RNAi or control L4440 RNAi and immunoprecipitated with an anti-FTT-2 antibody. Upper panel: immunoblotting with an anti-GFP antibody; middle panel: immunoblotting with an anti-FTT-2 antibody; lower panel: immunoblotting with an anti-actin antibody. Actin was included as a loading control for the input extracts.

Table 1

RNAi inactivation of *ftt-2* promotes dauer formation in *daf-2(e1370)* at 22°C.

	Gene inactivation by RNAi	L4440	*daf-2*	*daf-16*	*ftt-2*	*par-5*
daf-2 (e1370) at 22°C	% of worms in dauer stage	4.5%	100%	0%	99.5%	4.6%
	Total number of worms scored	334	214	423	184	328
N2 at 25°C	% of worms in dauer stage	0%	0.8%	0%	0%	0%
	Total number of worms scored	579	601	628	589	557

daf-2(e1370) mutant worms or N2 worms were exposed to the various RNAi bacteria starting as embryos and allowed to develop at the indicated temperature. Total number of worms scored and the percentage of worms remained in the dauer stage on day 4 (for *daf-2(e1370)*) or day 3 (for N2) are shown. *ftt-2* and *daf-2* RNAi dramatically enhances dauer formation in *daf-2(e1370)* at 22°C, whereas *par-5* RNAi behaves similarly to the L4440 control RNAi. However, neither *ftt-2* nor *daf-2* RNAi was able to significantly enhance dauer formation in N2 worms at 25°C.

Table 2

RNAi inactivation of *ftt-2* shortens the lifespan of N2 worms but has no effect on the lifespan of *daf-2(e1370)* worms.

		Mean (days)	Median (days)	# counted	P-value
N2	L4440 RNAi	15.200	15.000	36	N/A
	ftt-2 RNAi	11.665	11.000	46	0.000[a]
	par-5 RNAi	16.440	19.000	39	0.380[a]
	daf-2 RNAi	39.925	40.000	40	0.000[a]
	daf-16 RNAi	10.216	10.000	38	0.000[a]
daf-2(e1370)	L4440 RNAi	48.604	50.000	53	N/A
	ftt-2 RNAi	46.846	52.000	52	0.737[b]
	par-5 RNAi	50.533	52.000	60	0.764[b]
	daf-2 RNAi	45.644	50.000	45	0.980[b]
	daf-16 RNAi	12.705	11.000	42	0.000[b]

The lifespan of N2 or *daf-2(e1370)* worms treated with the indicated RNAi was determined at 22°C and the results of one representative experiment are shown.

[a] Compared to N2 worms fed with L4440 RNAi bacteria;

[b] Compared to *daf-2(e1370)* worms fed with L4440 RNAi bacteria.